Removal of Bismarck Brown G dye over composites of metalized copper oxide nanoparticles with nitrogen and activated carbons

Conference Paper · October 2021

CITATIONS
0

READS
15

1 author:

Abbas Jassim Lafta
University of Babylon
99 PUBLICATIONS **251** CITATIONS

SEE PROFILE

Removal of Bismarck Brown G dye over composites of metalized copper oxide nanoparticles with nitrogen and activated carbons

Removal of Bismarck Brown G dye over composites of metalized copper oxide nanoparticles with nitrogen and activated carbons

Reyam Kareem. Jabbar and Abbas Jasim Atiyah*

University of Babylon, College of science, Department of Chemistry, IRAQ.

Corresponding Author email: sci.abbas.jassim@uobabylon.edu.iq

Abstract:

The present work describes preparation of composites of iron metalized copper oxide nanoparticles (Fe/CuONPs) using co-precipitation method. Then new composites were prepared by combination of Fe/CuONPs with each of nitrogen and activated carbons(ACs). Activated carbons was both natural (AC1) and physically activated AC (AC2). This yielding tertiary systems N/Fe/CuONPs, AC1/Fe/CuONPs, and AC_2/Fe/CuONPs. These prepared materials were investigated using different techniques and analytical methods such as Fourier transform infrared spectroscopy (FTIR), X- rays diffraction (XRD) technique, BET specific surface area, Scanning electron microscopy (SEM), Atomic absorption spectroscopy (AAS), and CHN microelemental analysis. The adsorption ability of these materials was investigated via following removal of Bismarck Brown G dye (BBG) from simulated industrial wastewaters over a suspension of these prepared materials. Different adsorption parameters and conditions were investigated such as effect of weight of adsorbent, effect of adsorption temperatures, and effect of pH of the dye solution. Besides that, adsorption isotherms were undertaken involving applying each of Langmuir and Freundlich adsorption isotherms was undertaken. From the obtained results it was found that, the optimum removal efficiency for this dye was noted when using AC2/Fe/CuONPs as adsorbent under these conditions. Also from adsorption isotherms, it was found that, the results were more fitted with Langmuir adsorption isotherm.

Keywords: Copper oxide nanoparticles, Activated carbons, Polluted dyes removal, Composites materials.

1.Introduction

Nano materials are a part of materials that having particles with at least one dimension in Nano scale (1-100) nm. Due to their tiny particles, these materials exhibited unique and enhanced chemical and physical properties including, catalytic reactivity, thermal conductivity, biological activity, and non-linear optical action[1]. In last few decades and due to industrial revolution, high levels of environmental pollution were emerged including air, water, and soil pollution. In this context, water pollution was very important issue as many of industrial sources such as textiles factories, pharmaceutical, paper factories, fertilizers and food industries are using large quantities of water in their work including operation and painting systems[2]. So that, these factories are flaunted large amounts of their colored industrial wastewaters to the near environment. These colored wastewaters are containing different types of dyes, and azo dyes (-N=N-) seem to be problematic polluted dyes. These dyes are having a complicated rigid structure and due to that it is not easy to be fragmented

under normal atmospheric conditions. Generally, these dyes make numerous environmental pollution troubles as they are considered as carcinogenic materials and can release carcinogenic and toxic substances[3].

Upon these considerations, many researchers have been focused in how to remove or at least minimize the levels of pollution of industrial wastewaters with these dyes. In this context, many methods and techniques were applied to achieve this goal, including fleshly and chemical processes such as precipitation, sorption, air removal, and photo degradation methods [4,5]. Among these different methods, using adsorption and photocatalytic processes are seemed to be active methods to treat the proposed industrial wastewaters. Herein, semiconducting photocatalysts can be used effectively in this manner [6]. Different types of semiconducting oxides were applied in this fields such as TiO_2,ZnO, ZrO_2, CoO and Cr_2O_3. Copper oxide (CuO) is a semiconducting material with a moderate bandgap energy and it is used for photoconductive and photo thermal applications [7-9]. Nano crystalline CuO can be prepared using chemical method[10], sol-gel technique[11], electrochemical method[12], caloric rotting of precursors[13] and co-implantation of alloy and element ions [14]. CuO is a p-type semiconductor and it can be used in wide varieties of applications such as catalysis[15], solar cells[16], gas sensor[17], energy fuel storage[18]. The main drawback in using CuO, is the back electron transfer (recombination reaction). In order to overcome this point and improve its surface properties different methods can be applied to improve its surface properties such as metal and non-metal doping, and combination with other species to yield a composited materials.

The present work describes synthesis of CuO nanoparticles and then it would be modified via combination with metal and non-metal species to yield AC/N/Fe/CuONPs. Then the activity of these materials would be investigated via following removal of Bismarck brow G dye from its simulated industrials wastewaters applying different reactions conditions and parameters.

2. Experimental part:

2.1: Synthesis of Copper Oxide nanoparticles

CuO nanoparticles were prepared by precipitation method using copper chloride ($CuCl_2$) and copper nitrate ($Cu(NO_3)_2.3H_2O$). A solution of each of them (0.1 M) was prepared by dissolving each of them in 100 ml deionized distilled water. After that, NaOH solution (0.1 M) was gradually dropped with continuous stirring until pH reached to 14. Black precipitate was obtained and washed with deionized water and absolute ethanol for several times until reaching a pH around 7. Then it was dried at 80 °C for16 hr., and then it was calcinated at 500 °C for 4 hr[19].

2.2. Synthesis of metalized iron- copper oxide nanoparticles

A composite of Fe-doped/CuO was prepared using a hydrothermal method. According to this technique were taken different weight proportion of [Fe $(NO_3)_2.9H_2O$] 0.01, 0.03, 0.05 gram with 1gram of CuO (60:40%). These material were dissolved in 20 ml of deionized distilled water with sonication for 30 minute separately. Then, these were mixed together and sonicated for 20 minute. The obtained precipitate was separated and dissipated at 80 ^{O}C and then washed with deionized water and dried at 100 ^{O}C for 4 hr., and afterward calcinated at 250 ^{O}C for 3 hours[20,21].

2.3. Synthesis of activated carbons(AC1 and AC2)

Iraqi Barban dates palm seeds were collected from local market and it was used as starting materials to prepare the activated carbon. For all samples the seeds were washed with hot distilled water to remove dust and other waste impurities and then dried at 110 ºC for 2 hr. The dry seeds were grinded carefully to yield natural product which is designed as (AC1). Another sample was physically activated and the activation process was done by heating at 600 ºC in a graphite furnace for 1 hr.

under a nitrogen atmosphere. After heating, all the samples were cooled to room temperature and the resultant activated carbon designed as (AC2)[22].

2.4. Synthesis of a composite of N/Fe/CuONPs

Nanocomposite of Fe- doped CuO with Nitrogen was prepared using hydrothermal method. In this method, Fe/ ZnO NPs (1.0 g.) was suspended in 30 mL of DI-DW. A solution of NH_4Cl (0.03 g.) was suspended in 30 mL (DI-DW)with sonication for 30 minute. These two suspensions were mixed together with continuous stirring at 80 ^{O}C and until the dissolvable dissipated. The obtained solid was collected and dried at 100 ^{O}C for overnight[23].

2.5. Synthesis of composites of AC1/Fe/CuONPs and AC2/Fe/CuONPs Nanocomposite of Fe/ CuO with activated carbons with both natural (AC_1) and physically activated carbons (AC_2) was prepared using hydrothermal method. According to this method, Fe/ZnONPs(1.0 g.) w,as suspended in 30 mL of DI-DW. In another flask,(0.01 g.), of (AC1) and another flask was suspended in30 mL(DI-DW) with sonication for 30 minute. Then these two suspensions were mixed in one flask with continuous stirring at 80 ˚C until the solvent was evaporated completely. At that point, the obtained solid was gathered and dried at 100 ˚C for overnight.

2.6. Characterization of the synthesized materials

2.6.1. Powder X- rays diffraction (PXRD) The crystal structure of prepared materials was investigated using powder X-rays technique, Phillips X-ray diffraction with CuKα radiation (1.542 A., 40 KV, 30 MA), in the 2θ territory, 10-80 degrees. XRD6000, Shimadzu, Japan.

2.6.2. Fourier-transform infrared spectroscopy (FTIR).

The presence of surface functional groups at the surface of the prepared materials was investigated using Fourier-change infrared spectroscopy (FTIR). FTIR spectra for arranged materials were recorded utilizing a (SpactraIR-2, Perkin Elmer Instrument, USA). The investigated samples were measured within a range of (400-4000) cm^{-1} on a pallet with a KBr dose at room temperature[24].

2.6.3. Scanning electron microscopy (SEM)

Surface morphology of the prepared materials was investigated using scanning electron microscopy(SEM). The specimens were analyzed by a Scanning Electron Microscope (SEM, Zeiss , Germany) at electron high tension EHT .

2.6.4.Spesific surface area of the prepared materials Sares method can be used in estimation of surface area of porous materials. According to this method, 0.5 gm of specific materials is acidified with 0.1 M HCl to reach a pH(3-3.5). The volume then complete to a final volume of 50 mL with deionized DW. Then 10 g. of NaCl is added to this mixture. Then, titration is initiated with NaOH (0.1 M) in burette, in a thermostatic bath to keep temperature in the range of (298 ±0.5 K).Adjust the pH of mixture to pH=4, then start titration slowly and carefully to pH=9. Then record the volume (V) that is required to increase pH from 4 to 9.The surface area by Saers(S)[25] is:

$S(m^2/gm)= 32V-25$

2.6.5. Atomic absorption spectroscopy(AAS)

Doping of CuONPs with Iron was explored using atomic absorption spectroscopy utilizing Atomic absorption spectrophotometer phoenix-99986, UK. Using iron hallow cathode lamp as a source of radiation.

2.6.6. Microelemental analysis(CHN)

This unit analyzes various elements like carbon , nitrogen and hydrogen ,and it gives the ratio of these elements in organic compounds ,macro-organic metallic compounds ,clusters and polymers in solid or solution state. Screening of element C, H, an N was investigate using CHN micro elemental Analyses system GmbH VarioEL V5.19.9 23. Apr. 08, CHNS Mode, S. No.: 11086109 .

2.7. Adsorption ability of the prepared materials

The adsorption capacity of the synthesized was examined using a aqueous solution of BBG dye (150 mL, 50 ppm). In each run 0.05 g. of the materials was suspended in dye solution with continuous stirring at room temperature in dark. Then periodically, 5 mL of the reaction mixture were withdrawn and centrifuged carefully to insure removing of fine particles. The absorbance of the obtained supernatant liquid was recorded at 468 nm using UV-visible spectrophotometer UV-visible spectrophotometer (UV-1650PC Shimadzu, Japan). Then removal efficiency was determined using the following relation [26].

$$\boldsymbol{Removal}\ \% = \boldsymbol{A0} - \boldsymbol{At}/\boldsymbol{A0} \times \mathbf{100} \qquad (1)$$

A progression of experiments were carried out to determine the optimum reaction conditions optimum such as weight of catalytic and pH of the reaction mixture that can accomplish high removal efficiency for dye over the prepared nanocomposites materials, . To obtain an optimum used mass of the prepared composite (CuO:Fe 3%/AC_2), a dye solution with a concentration of 50 ppm was suspended with graduated masses of materials nanocomposite (0.01, 0.05, 0.10 , 0.15 g.). the optimum mass of nanocomposite can be evaluated. Then the same arrangement would be followed to evaluate optimum pH would be researched by performing a series of experiments with different pH values (pH =4, 6,7,8 and10). The pH values were adjusted at the desired level using NH_3or HNO_3solutions. The absorbance for the above solutions was measured at λmax = 468 nm, and the efficiency of removal effectiveness of this dye was determined using the relation that was referenced in equation(1)[27].

3. Results and Discussion

3.1. Powder X- rays diffraction (XRD)

XRD patterns for neat CuONPs and that doped with Fe 3% and AC2/Fe /CuO are presented in Figure 1. From this figure, XRD patterns for CuO are shown characteristic peaks at 2θ= 32, 35, 38, 48, 53, 58, 61, 65, 66,68, 72, and 75. XRD patterns of CuO doped with Fe 3% are shown peaks of both iron particles and peaks of CuO. From these patterns, some of these peaks are overlapped with that of CuO. From other hand, XRD patterns of the tertiary composite of AC_2/Fe /CuO are almost similar to that of binary system Fe/CuO. In general, it is clear that doping of CuO with both of Fe and AC_2 in these proportion does not affect significantly on its crystal structure and its peaks are almost like that of neat CuONPs. From the acquired results of XRD patterns for the prepared catalyst, it was found that there were some deviation in the positions of the peaks and d-spaces for standard values by coordinating with (JPCDS). This deviation is obtained by influencing between oxides[28].

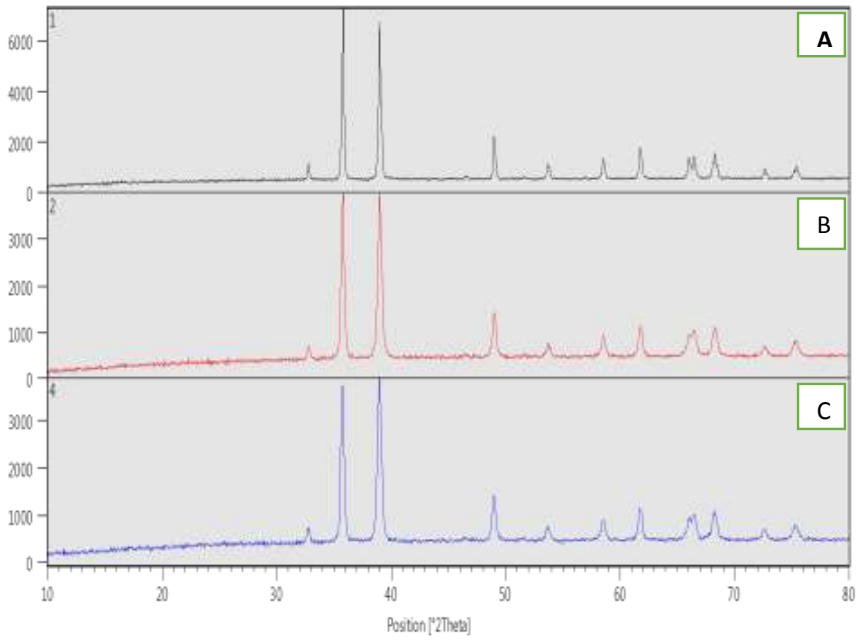

Figure 1. XRD patterns of neat CuO(A) , and Fe-doped CuO (B)andAC2/Fe/CuO(C) nanoparticles

3.2. Scanning electron microscopy(SEM)

Surface morphology of each Fe/CuO, AC1/Fe/CuO, AC2/Fe /CuO and N/Fe/CuO was explored using SEM. The surface morphology of neat Fe/CuONPs is shown in Figure 2.A, it shows moderately homogeneous spherical particles with a particle size around 31 nm which is consistent with that obtained from XRD designs applying Scherer's equation[29]. Images of AC2/Fe /CuO is shown in Figure 2,C, this image shows less homogeneity with relatively larger particle size as well as presence of particle agglomeration. This most likely emerges from the presence ofAC2 in the composite which can enhance surface synergetic effect that prompts increase of particle size because crystal growth under these conditions. Image of the composite N/Fe/CuO is shown in Figure 2-D, from this image it can be seen that there is a relatively shows homogeneous distribution with spherical particle that is almost similar to that of Fe/CuO but N/Fe/CuO show relatively larger particle size than that for Fe/CuO. This probably arises from crystal growth upon doping with nitrogen species.

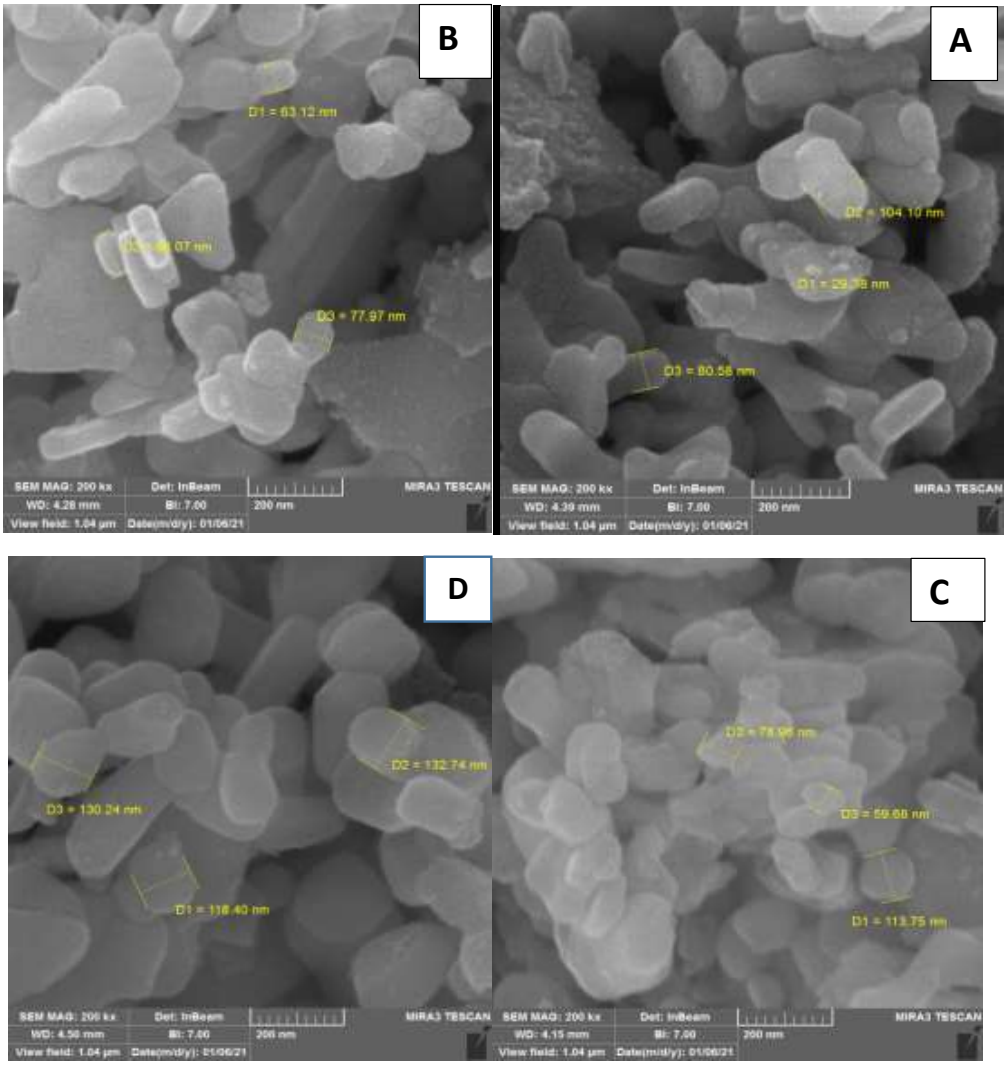

Figure 2. SEM images of (A)-Fe/CuO, (B)- composite AC1/Fe/CuO, (C)- AC2/Fe/ CuO and (D)-N/Fe/CuO.

3.3. Surface area of the prepared materials

The surface area of the prepared materials and composites was estimated using Saers method. The obtained results of specific surface areas are listed in Table1.

Table 1:Spesific surface area of the prepared materials

Material	Surface area (m^2/g.)
AC_2/Fe/CuO	343
AC_1/Fe/CuO	307
N/Fe/CuO	243
Fe/CuO	279

From these results it can be seen that, the composite AC2/Fe/CuO showed higher specific surface area and this probably arises from high porosity due to existence of activated carbons in the structure of this composite. A high porosity of AC2 is due to physically activation for this type of carbon species. While a composite AC1/Fe/CuO showed lower specific surface area, this probably due to low porosity of AC1 as compared with AC2 as it was combined in a composite as a natural product without pyrolysis activation. For composite N/Fe/CuO, it showed lower specific surface area in comparison with Fe/CuO. This is probably due to increasing of particles size of Fe/CuO upon doping with nitrogen. Increasing of particle size leads to reduce of specific surface area.

3.4. Fourier transform infrared spectroscopy(FTIR)

FTIR spectra of neat CuONPs, and Fe/CuO are shown in Figure3. These spectra show a characteristic peak of CuO at around 491 cm^{-1} which is a assigned to Cu-O bond , and the peak around 572 cm^{-1} which is assigned to vibration of Fe-O bond. The peaks around 1570 cm^{-1} is related to the asymmetric and symmetric stretching vibrations of carboxylic group originating from the reaction intermediates respectively[30]. The peaks around 2887 and 2896 cm^{-1}can be assigned to C−H vibration mode[31]. The broad peak around 3389 -3477 cm^{-1}in each of neat for Fe/CuO and AC2/Fe/CuO is related to O-H bond in both samples and water molecules have been absorbed by both nanocomposites[32]. Figure3,shows FTIR spectra for the tertiary composite (AC2/Fe /CuO). From these spectra , FTIR spectra of AC2/Fe/CuO show peaks around 1680-1640cm^{-1}, these are allocated to the vibration of -C=C- of alkenes at the surface. The peak around 1500-1400cm^{-1} is assigned to vibration of C-C bond in the aromatic ring at the AC surface. The peaks in the range of 1685-1627 cm^{-1}can be attributed to the vibration modes of C=O at the surface. The peak around 1296-1068cm^{-1} is assigned to stretching vibration of CO group at the surface of ACs.

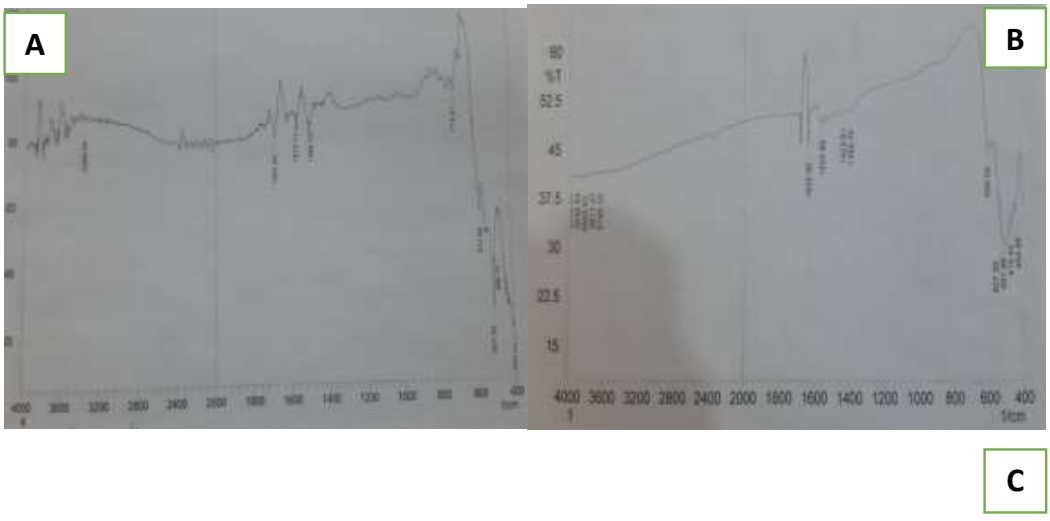

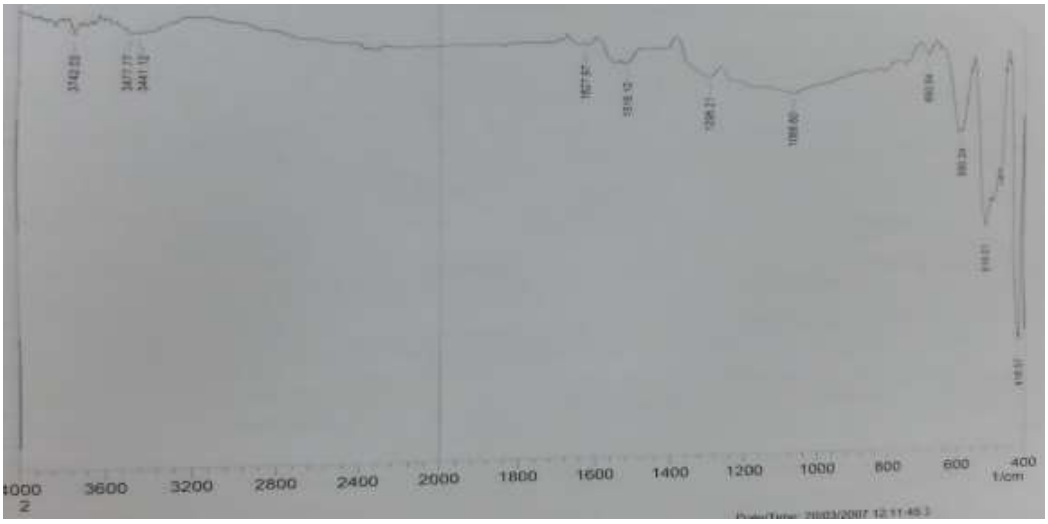

Figure 3:FTIR spectra for the tertiary composite (A)CuO and (B)Fe/CuO 3% and (c)AC2/Fe/CuO.

3.5.Atomic absorption spectroscopy (AAS)

To confirm presence of Fe in a composition of the composite AC2/Fe/CuO, atomic absorption spectroscopy was used to determine using iron hallow cathode lamp irradiation. According to this technique, it was found that the ratio of iron in the tertiary composite was around (0.21%).

3.6. CHN micro elemental analysis

Microelemntal analysis was performed to confirm presence of carbon and nitrogen species in the tertiary composites. The obtained results of CHN analysis, for the composite AC2/Fe/CuO , the value carbon was around (7.415) and nitrogen(0.393) hydrogen(0.150). For the tertiary composite N/Fe/CuO, the value of carbon was (0.333), nitrogen was around (0.251) and hydrogen was around (0.127). In general, these results are confirmed presence of these elements in the composition of these composites and are close to the ratios that were designed according to our procedure that were applied during preparation of these materials.

3.7. Adsorption ability of the prepared materials

The adsorption ability of the prepared composites N/Fe/CuO , AC1/Fe/CuO and AC2/Fe /CuO was investigated via following removal of BBG dye from its simulated industrial wastewaters by adsorption over composite. All experiments were performed using BBG dye concentration of 50 ppm, 150 mL, 0.15 g. and a pH 5 of dye solution. The acquired results of the adsorption BBG dye over prepared nano composite are shown in Figure 4. From these results it can be seen that, the best adsorption efficiency was seen over AC2/Fe /CuO in comparison with other adsorbents under the same adsorption conditions. This most likely emerges from high porosity of this tertiary composite in comparison with each of neat AC1/Fe/CuO and N/Fe/CuO with its higher BET surface area in comparison with different adsorbents that were utilized in this study[33].

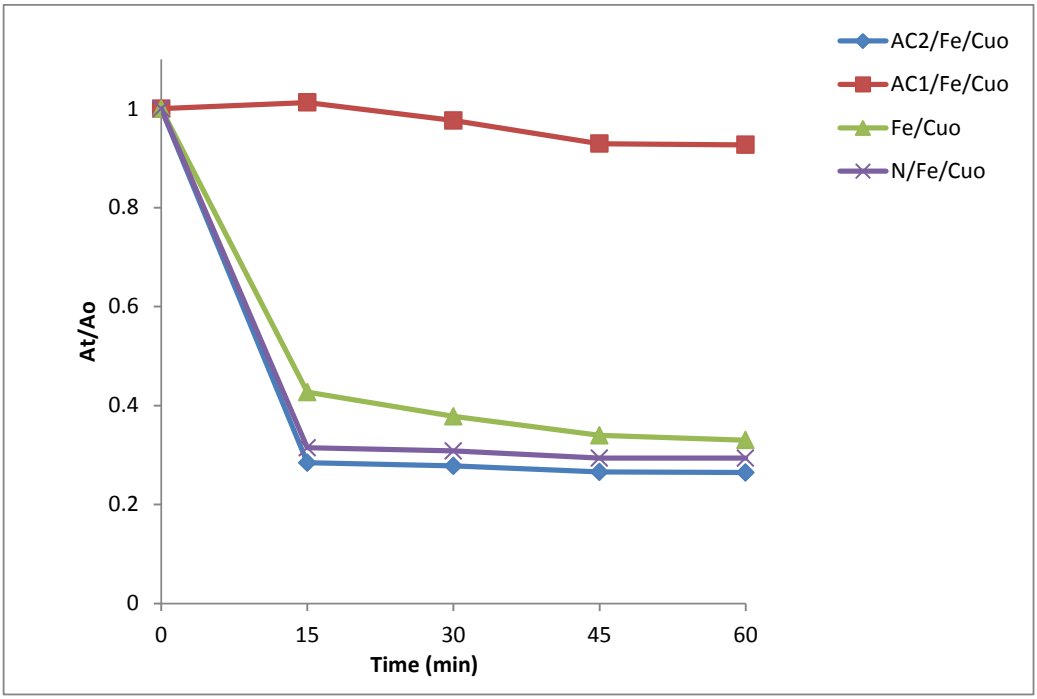

Figure 4: Adsorption efficiency of BBG dye over AC1/Fe/CuO, AC2/Fe/CuO, N/Fe/CuO, and Fe/CuO.

3.7.1. Effect of amount of adsorbent on BBG dye removal

In order to investigate effect of dose of the used adsorbent on the efficiency of dye removal from its simulated aqueous solution, a series of experiments were performed using different doses of AC2/Fe /CuO. These masses were 0.01, 0.05 and 0.10, 0.15, 0.20, and 0.25 g. These experiments were carried out under the same conditions with adsorption period of one hour for all runs. The adsorption ability was followed by recoding the absorbance of the supernatant liquid with measuring absorbance at 468 nm. From the obtained results, it was found that the dose 0.15 g. of the used composite(AC2/Fe/CuO) showed a best effectiveness of dye removal in comparison with other masse as shown in Figure 5. From the obtained results, it can be seen that, there was an increase in efficiency of dye removal with increase of dose of the used catalyst. This can be related to the increase of the available adsorption sites as the mass was increased of the used materials. This would lead to adsorb more dye molecules on the available adsorption sites. Upon using doses greater than 0.15 g., there was reduction in the efficiency of dye removal, this can be reasoned to increase density of the solution and aggregation of materials particles when using high doses of the adsorbent[33,34].

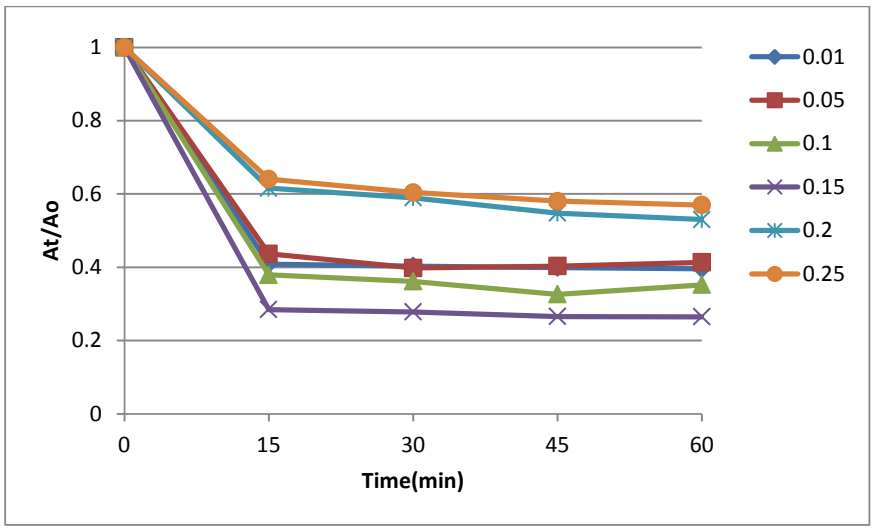

Figure 5:Effect of dosage AC2/Fe/CuO on the efficiency of removal of BBG dye by adsorption from its aqueous solution over the tertiary composite.

3.7.2. Effect pH of solution on BBG dye removal

To screening the impacts of pH of dye solution on its removal from an aqueous solution. Adsorption processes were performed under various pHs values for dye solutions (4,5,6,7, and 8). Adsorption processes were carried out by applying same adsorption circumstances for each run with change of pH of the dye solution. For each case, 0.15 g. of AC2/Fe/CuONPs was with 150 mL of 50 ppm dyes solution at 20ºC for one hour. The obtained results are presented in Figure 6 and from these results, it can be noted that, the optimum result of BBG dye removal was recorded at pH=5. At higher pH values more than this value , the surface of adsorbent becomes basic, this can lead to repulsion of dye molecules with adsorbent surface and hence leads to reduce efficiency of dye removal by adsorption. On the other hand, too acidic environment pH=4, showed low removal effectiveness in comparison with pH=5. This result can be attributed to effective attraction between dye molecules and the positively charged in the acidic medium. In basic mediums, a repulsion would occur between negatively charged surface and dye molecules, which leads to reduce the efficiency of dye removal under these conditions. From other hand, high acidic medium (pH>5) probably leads to strong electrostatic interactions which leads to reduce adsorption of dye molecules[35,36] .

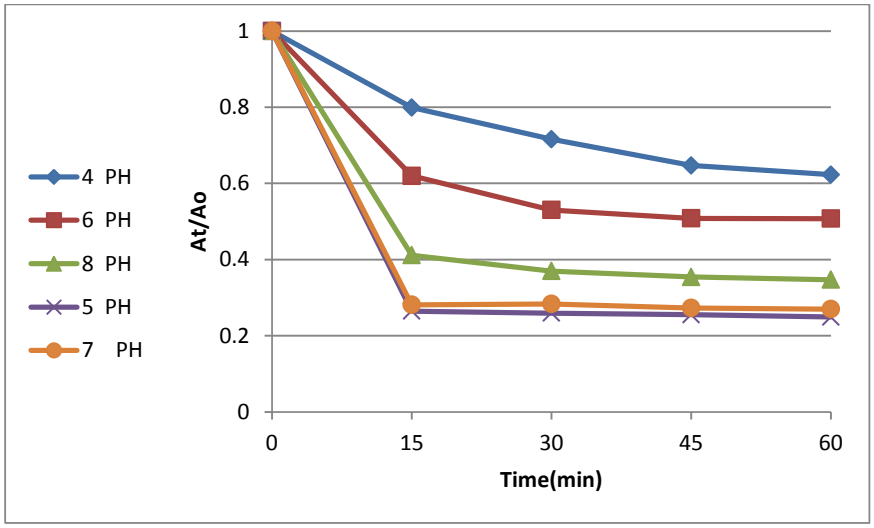

Figure 6. Effect of pH of reaction mixture on efficiency of adsorption of BBG dye over tertiary composite AC2/Fe/CuO.

3.7.3. Effect of temperature of reaction mixture on dye removal

The effect of reaction temperature on activity of adsorption of BBG dye over AC2/Fe/CuO was investigated via performing dye adsorption under various temperatures in the range from 288–308 K with increasing by five degrees for every increment with keeping other reaction conditions constant. These conditions involve using a dye in a concentration of 50 ppm in 150 mL, nano composite loading of 0.15 g., and the pH =5 of the reaction mixture. The obtained results are shown in Figure 7. From these results, it was found that the effectiveness of dye removal was enhanced with increasing of adsorption temperature and the best removal efficiency was recorded at 308 K. An increase in temperature leads to increase in diffusion rate of dye molecules from the bulk solution to adsorbent active sites on the surface. At higher temperatures, greater than 308 K, any increase in reaction temperature can affect the amount of adsorbed molecules at the surface and increase the rate of desorption of dye molecules away from the surface. This effect leads to reduce the efficiency of dye removal under these conditions [37,38].

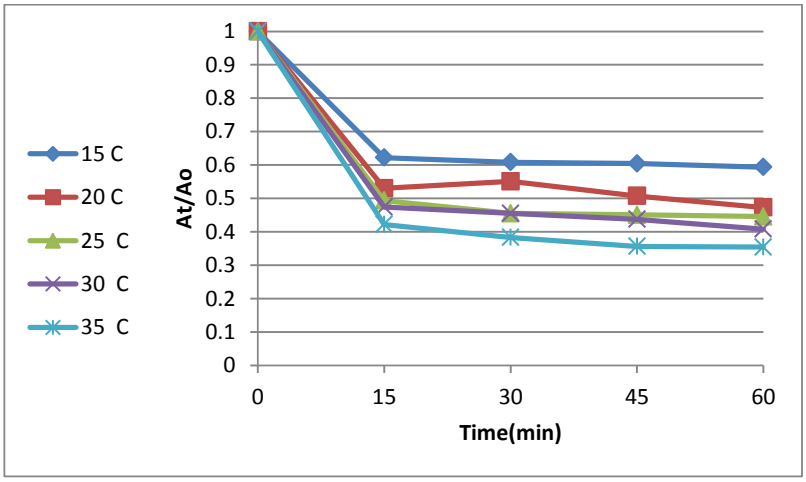

Figure.7: Effect of temperature on removal efficiency of BBG over nanocomposite AC2/Fe/CuO.

3.7.4. Adsorption isotherms

Adsorption isotherms were investigated by applying Langmuir and Freundlich equilibrium models. where qe is the amounts of the BBG adsorbed at equilibrium (mg/gm) and at time t (min), Ce is the concentration of adsorbate(mg/L) in the solution at equilibrium. Qm, refers to capacity of monolayer adsorption of BBG dye in (mg/g); KL and KF refer to Langmuir and Freundlich adsorption constant in (L/mg). Generally, maximum adsorption capacity for composite was estimated using Langmuir and Freundlich isotherms. This was conducted by applying reaction conditions, reaction temperature of temperature 25 ºC, pH 5.0, and the initial concentration of dispersed dye 50 ppm. The doses of the used composite ranged from 0.01, 0.05, 0.10 and 0.15 g. These isotherms are presented in Figures. 8 and 9 and the obtained data are shown in Table 2.

Isotherms	Parameters	Values
Freundlich	KF	9.7711
	n	1.9319
	R^2	0.8737
Langmuir	Qm	39.2156
	KL	0.0465
	R^2	0.9451

Table-2 :Adsorption constants for both Langmuir and Freundlich adsorption isotherm

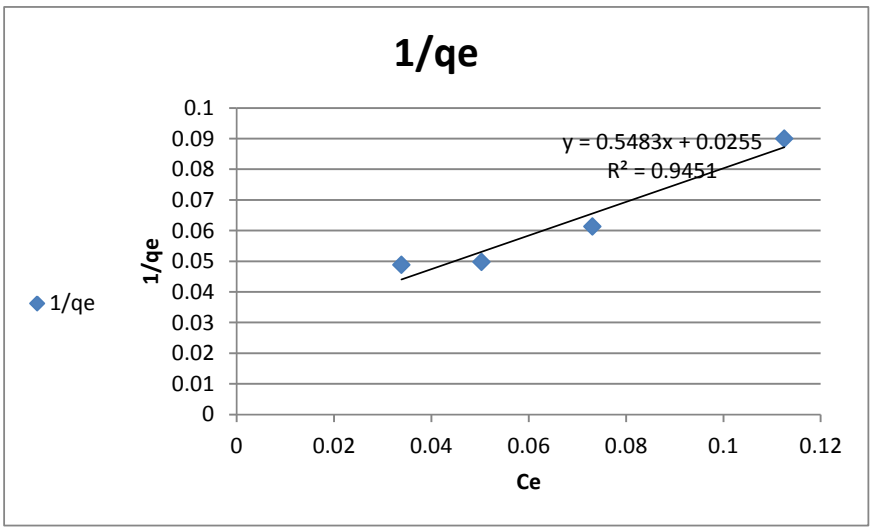

Figure.8: Langmuir adsorption isotherm for adsorption of Bismarck brown G on the prepared catalyst

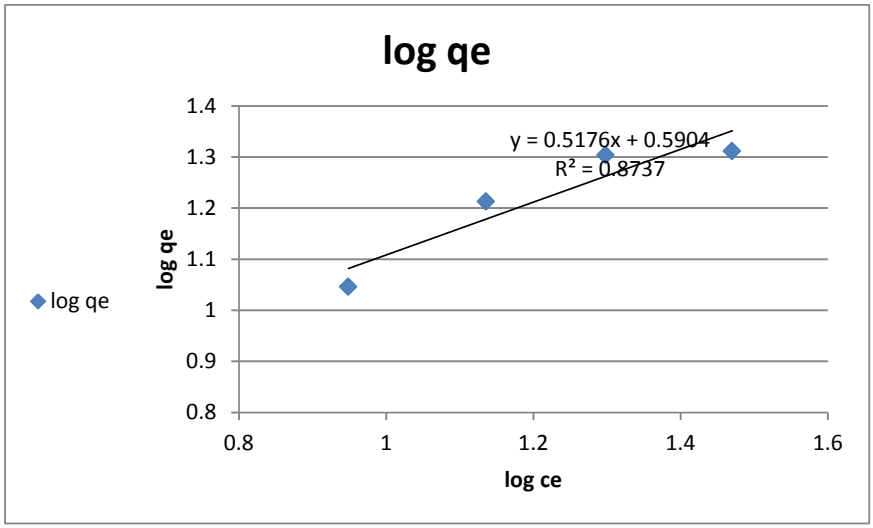

Figure.9: Freundlich adsorption isotherm for adsorption of Bismarck brown G over the catalyst

From the obtained results of Langmuir and Freundlich adsorption isotherms, it can be seen that, the value of the rectification factor (R^2) that are acquired from Langmuir model is more than that for Freundlich isotherm. For this case, adsorption isotherms seem to be fitted with Langmuir adsorption model rather than Freundlich isotherm[38]. In this manner, it can be conclude that adsorption processes were occurred according to chemical adsorption mechanisms. This investigation is boosted from the results of effect of temperature on adsorption processes as adsorption efficiency was increased with increase in temperature of adsorption processes[39,40].

3.8. Conclusions

In this work, CuO nanoparticles have been successfully synthesized by environmentally friendly method which known as black approach. The obtained results showed that, the optimum result of BBG dye removal by adsorption was noted when using a tertiary composite of AC2/Fe /CuO. For this composite the best removal efficiency was recorded under a pH= 5 of dye solution, a mass of adsorbent of 0.15 g. and adsorption temperature 308 K.

References :

[1] A.Teragundi, and T. Nanjundeswaraswamy, Literature Review on Synthesis of ZnO Nano Particles Using Natural and Synthetic Methods. Int. J. Res. Sci. Innov. |V, 67–71 ,2018.
[2] Iino. K., Kitano. M., Takeuchi Matsuoka.M., and Anpo .M, M, Curr. Apple. Phys., 6, 982. Ladakowicz. L., Solecka .M., and Zylla .R. (2001). J. Biotechnol. 89, 175, 2005.
[3] Toma. F.L., Bertrand. G., Chaw. S.O, D., Klein. H., Liao. C., Meunier, and Oddet. C.C., Mater Sci. Eng., 56 , 417, 2006.
[4] Robinson. T.F., McMullan. Marchant .G., and Nigam. R., Bioresour. Technol., 77, 247, 2001.
[5] Georgiou D., Melidis. P., Aivasidis. A., Gimouhopoulos. K. Dyes Pigments, Grenoble, D.C., Estadt M.M., and Ollis .D.F., Journal of Catalysis, 67(1), 90-102,2002.
[6] Farrauto. R.J., C.H. Bartholomew. (1997). Fundamentals of Industrial Catalytic Processes, Chapman & Hall, Kluwer Academic Publishers, London, Chapter 5.
[7] A.E. Rakhshani, Solid-State Electron. 29, 7, 1986.
[8] M.K. Wu, J.R. Ashburn, C.J. Torng, P.H. Hor, R.L. Meng, L. Gao, Z.J. Huang, Y.Q. Wang, and C.W. Chu, Phys. Rev. Lett., 58, 908 , 1987.
[9] A.E. Rakhshni, Solid State Electron., 29, 7, 1986.
[10] Salam Hussein Ewaid et al 2020 J. Phys.: Conf. Ser. 1664 012143.
[11] R.V. Kumar, Y. Diamant, and A. Gedanken, Chem. Mater., 12, 2301,2000.
[12] 11. A. A. Eliseev, A.V. Lukashin, A. A. Vertegel, L.I. Heifets, A. I. Zhirov, and Y. D. Tretyakov, Mater. Res. Innov., 3, 308, 2000.
[13] 12. K. Borgohain, J.B. Singh, M.V. Rama Rao, T. Shripathi, and S. Mahamuni, Phys. Rev., 61, 11093, 2000.

[14] Salam Hussein Ewaid et al 2021 IOP Conf. Ser.: Earth Environ. Sci. 722 012008
[15] 13. J.Q. Yu, Z. Xu, D.Z. Jia, and Chin. J., Func. Mater. Instrum., 5, 267, 1999.
[16] 14. S. Nakao, M. Ikeyama, T. Mizota, P. Jin, M. Tazawa, Y. Miyagawa, S. Miyagawa, S. Wang, and L. Wang, Rep. Res. Cent. Ion Beam Technol., 18, 153, 2000.
[17] 15. Jianliang C Yan, W Tianyi, Ma Yuping Liu, and Zhongyong Yuan, Synthesis of porous hematite nanorods loaded with Cuo nanocrystals as catalysts for CO oxidation, J. Nat. Gas Chem., 20, 669-676, 2011.
[18] Salam Hussein Ewaid et al 2021 IOP Conf. Ser.: Earth Environ. Sci. 790 012075
[19] Jess K, Nicolas G, Richard R, Eric Miller. Advances in copper-chalcopyrite thin films for solar energy conversion, Sol Energ. Mat. Sol. C, 94,12-16,2009.
[20] Yang Z, Xiuli He, Jianping L, Huigang Z, and Xiaoguang G., Gas-sensing properties of hollow and hierarchical copper oxide microspheres, Sensor,128:293- 298, 2007.
[21] Bohr R H, Chun S Y, Dau C W, Tan J T, and Sung J, Field emission studies of amorphous carbon deposited on copper nanowires grown by cathodic arc plasma deposition, New Carbon Mater., 24,97-101, 2009.
[22] Kankanit Phiwdanga, Sineenart Suphankija, Wanichaya Mekprasarta, and
[23] Wisanu Pecharapaa,b , Synthesis of CuO Nanoparticles by Precipitation Method Using Different Precursors, Energy Procedia, 34,740 - 745, 2013.
[24] W. Keiko, A. Raymond Wong, S. Haryo Oktaviano, F. Takuya, N.Takuro, K. Koji and Y.Koichi, Energy & Environmental Science, 1-3, 2013, DOI: 10.1039/x0xx00000x, 2013.
[25] Y. Nosaka, M. Matsushita, J. Nishino, and A. Y. Nosaka, ―Nitrogen-doped titanium dioxide photocatalysts for visible response prepared by using organic compounds,‖ Sci. Technol. Adv. Mater., 6(2), pp. 143–148, 2005.
[26] Ahmed F. Halbus, Abbas J. Lafta, Zahra H. Athab and Falah H. Hussein, Asorption of reactive yellow dye 145 from wastewater onto Iraqi Zahdy and Khestawy date palm seeds activated carbons, Asian Journal of Chemistry, Volume 26, (176-172), 2014.
[27] B. Kahdum, A. Lafta and A. Johdh, Enhancement photocatalytic activity of spinel oxide(Co, Ni) 3O4 by combination with carbon nanotubes,Polish Journal of Chemical Technology, 19(3), 61- 67, 2017.
[28] A. Monshi, M. Foroughi, and M. Monshi, Modified Scherrer Equation to Estimate More Accurately Nano-Crystallite Size Using XRD,‖ World J. Nano Sci. Eng., 2(3), 154-160, 2012.
[29] R. A. Shawabkeh and M. F. Tutunji, Experimental Studies and Modeling of the basic dye Sorption by diamaceous clay, Applied Clay Sci., 24, 111-114, 2003
[30] A. Ameri, and A. Esrafily, Synthesis and properties of Fe_3O_4-activate carbon magnetic nanoparticles for removal ofaniline from aqueous solution: equilibrium, kinetic and thermodynamic studies, Iranian Journal of Environmental Health Sciences & Engineering, 10(19), 1-9.2013.
[31] E. Mohammad, M. Kareem, and A. Lafta, Preparation of MWCNTS/Cr2O3-nio nanocomposite for adsorption and photocatalytic removal of bismarck brown g dye from aqueous solution,‖ Indones. J. Chem., 20(3), 554–566, 2020.
[32] K. Sanchai and Y.H. Hang, Ind. Eng. Chem. Res., 50, 2015, 2015.
[33] https://doi.org/10.1021/ie101249r.
[34] R. Kabir, A. K. Saifullah, A. Z. Ahmed, and S. Masum, Synthesis of N-Doped ZnO Nanocomposites for Sunlight Photocatalytic Degradation of Textile Dye Pollutants, Journal of composite Science, 4(49), 1-10, 2020.
[35] S. Mofokeng, V. Kumar, R. Kroon, and O. Ntwaeaborwa, ―Structure and optical properties of Dy 3 + activated sol-gel ZnO-TiO_2nanocomposites, J. Alloys Compd.,71, 121-131, 2017,.
[36] B. Singh, V. Choudhary., S. Teotia, T. Gupta, V. Singh, S. Dhakate and R. B.Mathur, Solvent free, efficient, industrially viable, fast dispersion process based amine modified MWCNT reinforced epoxy composites of superior mechanical properties, Adv. Mater. Lett., 6(2), 104-113, 2015..
[37] A. Subramaniyan, V. Visweswaran, C. Kumar, and T. Sornakumar, Preparation and Characterisation of ZnO - SiO_2 and Bi_2O_3 - CuO, Nanocomposites, 3(1), 79–84, 2018.
[38] S. Kaniyankandy, S. Verma, J. Mondal, D. Palit, and H. Ghosh, Evidence of Multiple Electron Injection and Slow Back Electron Transfer in Alizarin-Sensitized Ultrasmall TiO_2 Particles, J. Phys. Chem. C,113(9), 3593–3599.2009.
[39] K. Mahmodi, K. Hasni, N. Hamdi, and E. Srasra,Density measurement and equal density temperature of CO2 + brine from Dagang - formation from 313 to 363 K, Korean J. Chem. Eng., 32(2), 274,2015.
[40] 35. A. Jorfi,S. Mirali,, A. Mostoufi, and M. Ahmadia,Visible Light Photocatalytic Degradation of Azo Dye and a Real Textile Wastewater Using Mn, Mo, La/TiO2/AC Nanocomposite,Chem. Biochem. Eng. Q., 32(2), 215–227, 2018.

[41] U. Alam, A. Khan, W. Raza, A. Khan, D. Bahnemann, and M. Muneer, Highly efficient Y and V co-doped ZnOphotocatalyst with enhanced dye sensitized visible light photocatalytic activity, Catalysis Today, 284, 169-178, 2017.
[42] Ahmed Alaa Kandoh et al 2021 IOP Conf. Ser.: Earth Environ. Sci. 790 012073
[43] Ewaid, S.H.; Abed, S.A.; Al-Ansari, N.; Salih, R.M. Development and Evaluation of a Water Quality Index for the Iraqi Rivers. Hydrology 2020, 7, 67.
[44] Ewaid, S.H.; Abed, S.A.; Al-Ansari, N. Water Footprint of Wheat in Iraq. Water 2019, 11, 535.
[45] Ewaid, S.H.; Abed, S.A.; Al-Ansari, N. Crop Water Requirements and Irrigation Schedules for Some Major Crops in Southern Iraq. Water 2019, 11, 756.
[46] Soares, E.T., Lansarin, M.A., and Moro, C.C., A study of process variables for the photocatalytic degradation of rhodamine B, Braz. J. Chem. Eng., 24 (1), 29-36, 2007.
[47] K.A. Kusmierek and A. Swiatkowski, Pol. J. Chem. Technol., 17, 23 (2015); https://doi.org/10.1515/pjct-2015-0005.
[48] Emman J. Mohammad, Mohanad M. Kareem, and Abbas J. Atiyah, Preparation of MWCNTS/Cr2O3-NiO Nanocomposite for Adsorption and Photocatalytic Removal of Bismarck Brown G Dye from Aqueous Solution, Indones. J. Chem., 20(3), 554 – 566,2020. 40. Tor N., Danaoglu G., and Y. Cngeloglu, Removal of fluoride from water by using granular red mud: batch and columns studies, Journal of Hazard Materials, 164, 271-287, 2009.
[49] Salah, A. (2020). The New Combination of Semi-Analytical Iterative Method and Elzaki Transform for Solving Some Korteweg-de Vries Equations. Al-Qadisiyah Journal Of Pure Science, 25(1), Math. 23 - 26.
[50] Sami Abd ali , mohammed, Shaker Hussein, A., & mohammed hadi, H. (2020). Study The Current Density-Voltage (J-V) Characteristics of α-Fe2O3 Thin Film Prepared by Spray Pyrolysis Technique. Al-Qadisiyah Journal Of Pure Science, 25 (1), Phys 1-7.